Feedback Stabilization of Resistive Wall Modes in the Presence of Multiply connected Wall Structures

P. Merkel, M. Sempf

Max-Planck-Institut für Plasmaphysik, Garching, Germany, EURATOM Association

e-mail contact of main author: peter.merkel@ipp.mpg.de

Abstract. The feedback stabilization of resistive wall modes (RWMs) for realistic wall structures has been studied splitting the problem in two parts. In the open-loop part, the complete set of eigenvalues and eigenfunctions of the plasma-resistive wall system without feedback currents has been determined. Then, in the closed-loop part an initial value problem has been formulated for the time evolution of the RWMs and the currents of the feedback coils. The feedback logics controlled by a set of free parameters prescribes the interaction between the feedback currents and the RWMs. After choosing their values, the effectiveness of the feedback can be studied by solving the characteristic equation of the closed-loop system. The procedure has been implemented numerically (STARWALL code) and applied to a resistive wall configuration for ASDEX Upgrade. For an optimal choice of the feedback parameters, the OPTIM code has been developed which optimizes the stability of a truncated closed loop system under variations of the free parameters.

1. Introduction

An external kink mode of an MHD equilibrium can be stabilized by a perfectly conducting wall sufficiently close to the plasma. In case of a real wall with non-zero resistivity the mode becomes unstable and grows on the resistive timescale of magnetic field diffusion through the wall. The growth rate of the resistive wall mode is typically orders of magnitude smaller than the kink mode in the no-wall case so that the stabilization of the RWM by an active feedback system becomes feasible. There are numerous publications on that topic, e.g. [1] and references therein. In this paper, the method published by Chu et al. [1] has been extended so that RWMs of 3D equilibria and their feedback stabilization in the presence of multiply connected wall configurations can be studied. The problem has been separated in two parts, namely, the open-loop and the closed-loop problem. In the open-loop part, the complete set of eigenfunctions of the plasma-resistive wall system has been determined. The feedback coils are included in the resistive wall configuration. They are additional passive resistive elements without an applied external voltage. The open-loop system is self-adjoint and one obtainss a complete set of orthonormal eigenfunctions.
The closed-loop problem can be formulated by including sensor loops and the feedback logics. The sensors measure the perturbed magnetic field at appropriate locations and the feedback logics relates the sensor signals to the voltages applied to the feedback coils. One gets an initial value problem for the time evolution of the RWMs and the feedback currents. The effectiveness of the feedback can be studied by solving the characteristic equation of the system. In order to find an optimal choice for the free parameters (gain matrix) of the feedback logics, a nonlinear optimization procedure has been developed minimizing the largest real part of the closed-loop eigenvalues. In Section 2, the open- and closed-loop problem and the optimization method are described. In Section 3, an application for ASDEX Upgrade is presented.

2. Solution method

An energy principle holds for the open-loop system. Assuming the RWM to be sufficiently slow the kinetic energy of the plasma perturbation can be neglected. The potential energy $W_p(\xi,\xi)$ of the perturbed plasma and the vacuum energy functional W_s have to satisfy

$$W_p(\xi,\xi)+W_s=0,\ W_s=\frac{1}{2}\int_{S_1} df\ (\mathbf{n}\cdot\xi)(\mathbf{B}\cdot\mathbf{B_0}) \tag{1}$$

with plasma-vacuum interface S_1, displacement vector ξ, equilibrium magnetic field $\mathbf{B}_0$, perturbed vacuum magnetic field $\mathbf{B}$ and exterior normal $\mathbf{n}$. The potential energy of the plasma perturbed by the displacement ξ is given by

$$\begin{aligned} W_p(\xi,\xi) &= \frac{1}{2}\int_{S_1} d^3r[\mathbf{C}^2+\Gamma p(\nabla\cdot\xi)^2-\mathcal{A}(\xi\cdot\mathbf{n})^2], \quad \mathbf{B}_0=\nabla s\times\nabla(F'_P\,v-F'_T\,u) \\ \mathbf{C} &= \nabla\times(\xi\times\mathbf{B}_0)+(\xi\cdot\mathbf{n})\mathbf{j}\times\mathbf{n}, \qquad\qquad \mathcal{A}=2(\mathbf{j}\times\mathbf{n})\cdot(\mathbf{B}_0\cdot\nabla)\mathbf{n}. \end{aligned} \tag{2}$$

provided by the CAS3D code [2], which computes internal and external eigenmodes of 3D MHD equilibria. The code uses flux coordinates s,u,v, where $s:\ 0\le s\le 1$ labels the magnetic surfaces and $(u,v):0\le u,v\le 1$ are poloidal and toroidal magnetic coordinates on the surfaces. F'_P, F'_T are the derivatives of the poloidal and toroidal flux with respect to s. The displacement vector is expanded in (u,v)-Fourier space:

$$\xi(s,u,v)=\sum_{\substack{m=0,n=1\\ m>0,n=-nf}}^{mf,nf} \xi^s(s)_{mn}\sin 2\pi(mu+nv)+\xi^c(s)_{mn}\cos 2\pi(mu+nv). \tag{3}$$

With respect to the flux coordinate s, the Fourier harmonics $\xi^s(s)_{mn}, \xi^c(s)_{mn}$ are discretized by a finite element method.

The term W_s in (1) corresponds to the energy flux accross the plasma-vacuum interface. The perturbed magnetic field $\mathbf{B}$ has to satisfy Maxwell's equations $\mathbf{B}=\nabla\times\mathbf{A},\ \nabla\times(\nabla\times\mathbf{A})=0,\quad \nabla\cdot\mathbf{A}=0$ and boundary conditions at the plasma-vacuum interface and the conducting wall. $\mathbf{A}$ is the vector potential. In case of a resistive wall, the boundary condition follows from Faraday's and Ohm's law: $\mathbf{E}+\frac{\partial\mathbf{A}}{\partial t}=0,\ \sigma\mathbf{E}=\mathbf{J}$. Assuming a time dependence $e^{\gamma t}$, one gets in the thin wall approximation the boundary condition

$$\mathbf{n}\times\mathbf{A}=\begin{cases} -(\mathbf{n}\cdot\xi)\mathbf{B}_0 & : \quad \text{on} \quad S_1 \text{ (plasma-vacuum interface)} \\ -\frac{1}{\sigma d\gamma}\mathbf{n}\times\mathbf{j}_2 & : \quad \text{on} \quad S_2 \text{ (resistive wall)}, \end{cases} \tag{4}$$

where $\mathbf{j}_2$ is the current in the resistive wall and σd is the surface resistance of the wall.
($\sigma=$ conductivity, $d=$ wall-thickness)

The vector potential $\mathbf{A}$ can be generated by surface currents $\mathbf{j}_1,\mathbf{j}_2$ on the plasma-vacuum interface, the resistive wall and feedback coils:

$$\mathbf{A}=\frac{1}{4\pi}\sum_{i=1}^{2}\int_{S_i} df_i\ \frac{\mathbf{j}_i}{\mid\mathbf{x}-\mathbf{x}_i\mid}+\frac{1}{4\pi}\sum_{l=1}^{n_c} I_l^c\int_{C_l} df_l\ \frac{\mathbf{v}_l}{\mid\mathbf{x}-\mathbf{x}_l\mid} \tag{5}$$

with $\mathbf{v}_l=$ normalized current density, $I_l^c=$ coil current, $n_c=$ number of coils. The currents have to be determined such that the boundary conditions for $\mathbf{A}$ on S_1 and S_2 are fulfilled. To solve cases with multiply connected wall configurations, a finite element method has been applied using a variational procedure.

One introduces the functional

$$\mathcal{L} = \frac{1}{8\pi}\sum_{i,k=1}^{2,2}\int_{S_i} df_i \int_{S_k} df_k \, \frac{\mathbf{j}_i\cdot\mathbf{j}_k}{\mid \mathbf{x}_i-\mathbf{x}_k \mid} + \frac{1}{2\gamma}\int_{S_2} df_2 \, \frac{\mathbf{j}_2\cdot\mathbf{j}_2}{\sigma d} + \int_{S_1} df_1 \, (\mathbf{n}\cdot\xi)\, \mathbf{n}\cdot(\mathbf{j}_1\times\mathbf{B}_0) \quad (6)$$

$$+ \frac{1}{8\pi}\sum_{l,l'=1}^{n_c,n_c} I_l^c I_{l'}^c \int_{C_l} df_l \int_{C_{l'}} df_{l'} \, \frac{\mathbf{v}_l\cdot\mathbf{v}_{l'}}{\mid \mathbf{x}_l-\mathbf{x}_{l'} \mid} + \frac{1}{4\pi}\sum_{l,i=1}^{n_c,2} I_l^c \int_{C_l} df_l \int_{S_i} df_i \, \frac{\mathbf{j}_i\cdot\mathbf{v}_l}{\mid \mathbf{x}_i-\mathbf{x}_l \mid}$$

$$+ \frac{1}{2\gamma}\sum_{l=1}^{n_c} R_l I_l^{c2} \int_{C_l} df_l \mathbf{v}_l^2 + \frac{1}{\gamma}\sum_{l=1}^{n_c} I_l^c \, U_{c,l}^{feedb}.$$

Divergence-free surface currents can be derived from current potentials: $\mathbf{j}_i = \mathbf{n}\times\nabla\phi^i,\ i=1,2$. The variation of $\mathcal{L}$ with respect to ϕ^1,ϕ^2 gives the correct boundary conditions for $\mathbf{B}$ at the plasma-vacuum interface and the wall. The open-loop problem is solved including the feedback coil currents as passive elements ($U_{c,l}^{feedb}=0$). The feedback coils are modeled as thin ribbon-like conductors of finite width. Replacing the $\mathbf{j}_i$ in $\mathcal{L}$ by the current potentials, the independent variables of the system are ϕ^1,ϕ^2 and I_l^c. For the finite element procedure the plasma-wall interface, the resistive wall and the feedback-coils are discretized into triangles. A triangle consists of the set of points given by

$$\mathbf{x} = \mathbf{x}_1 + \alpha\,\mathbf{x}_{21} + \beta\,\mathbf{x}_{31},\ \ 0<\alpha+\beta<1,\ \ \mathbf{x}_{ik}=\mathbf{x}_i-\mathbf{x}_k,\ \ i,k=1,2,3. \quad (7)$$

The surface-current density is assumed to be constant on the triangle and can be written as

$$\mathbf{j}_\Delta = \frac{\phi_1\,\mathbf{x}_{23}+\phi_2\,\mathbf{x}_{31}+\phi_3\,\mathbf{x}_{12}}{|\mathbf{x}_{21}\times\mathbf{x}_{32}|}. \quad (8)$$

The ϕ_i are the values of the current potential at the vertices of the triangles and they are the independent variables of the discretized functional $\mathcal{L}$. The contribution of a pair of triangles to the functional $\mathcal{L}$ is given by

$$\mathcal{L}_{\Delta\Delta'} = \frac{1}{8\pi}\mathbf{j'}_\Delta\cdot\mathbf{j}_\Delta\int_{\Delta'} df'\int_\Delta df\,\frac{1}{\mid \mathbf{x'}-\mathbf{x} \mid} \quad (9)$$

Two integrations of the fourfold integral are performed analytically, the remaining two are computed numerically. In order to compute the term determining the boundary condition at the plasma-wall interface,

$$\mathcal{L}(\mathbf{j}_1,\xi) = \int_{S_1} df_1\,(\mathbf{n}\cdot\xi)\,\mathbf{n}\cdot(\mathbf{j}_1\times\mathbf{B}_0) \quad (10)$$

one has to adjust the spectral discretization of the plasma perturbation to the finite element discretization of the vacuum part. There are two representations for the plasma-wall interface. For the plasma part, a Fourier expansion in (u,v) is used, while for the vacuum part the surface is discretized into triangles such that the vertices coincide with the mesh-points (u_i,v_k) used for the Fourier transform. With

$$\xi\cdot\nabla s = \sum_{\substack{m=0,n=1\\ m>0,n=-nf}}^{mf,nf} \xi_{mn}^s \sin 2\pi(mu+nv) + \xi_{mn}^c \cos 2\pi(mu+nv) \quad (11)$$

and

$$\mathbf{j}_1 = \mathbf{n}_1\times\nabla\phi^1,\quad ,\phi^1 = J_p\,u + I_p\,v + \phi^p(u,v), \quad (12)$$

one gets

$$\begin{aligned}\mathcal{L}(\mathbf{j}_1,\xi) &= (F_P' J_p - F_T' I_p)\,\xi_{00} + \sum_{m,n} 2\pi(nF_T{}' + mF_P{}')(\xi^s_{mn}R^c_{mn} - \xi^c_{mn}R^s_{mn}),\\ R^c_{mn} + i\,R^s_{mn} &= \frac{1}{n_u n_v}\sum_{j=0,k=0}^{n_v-1,n_u-1}\phi^p(\frac{j}{n_u},\frac{k}{n_v})\exp 2\pi i\,(m\frac{j}{n_u}+n\frac{k}{n_v}),\end{aligned} \tag{13}$$

where $J_p,\ I_p$ are the net toroidal and poloidal perturbed plasma currents driving the ξ_{00} mode. The remaining terms of the Lagrangian $\mathcal{L}$ can be discretized accordingly. The variables are the displacement ξ, the current potentials on the plasma-vacuum interface and the resistive wall and the feedback currents. The discretized variables are noted as follows: $X = \{\xi^s(s_i)_{mn},\ldots,\xi^c(s_i)_{mn},\ldots\}$ consists of all components of the displacement vector except of the normal components at the plasma boundary which are denoted by $\xi = \{\xi^s(1)_{mn},\ldots,\xi^c(1)_{mn},\ldots\}$ The current potential on the plasma-wall interface, on the resistive wall, and the feedback currents are denoted by $\Phi^p = \{\phi^1_1,\phi^1_2,\ldots\}, \Phi^w = \{\phi^2_1,\phi^2_2,\ldots\}, I^c = \{I^c_1, I^c_2,\ldots\}$ respectively..

Varying the discretized eq. (1) one obtains

$$\begin{pmatrix}\mathbf{M}_{XX} & \mathbf{M}_{X\xi}\\ \mathbf{M}_{\xi X} & \mathbf{M}_{\xi\xi}\end{pmatrix}\cdot\begin{pmatrix}X\\ \xi\end{pmatrix} - \begin{pmatrix}0\\ M_{\xi p}\,\Phi^p + M_{\xi w}\,\Phi^w + M_{\xi c}\,I^c\end{pmatrix} = 0 \tag{14}$$

From the discretized Lagrangian $\mathcal{L}$ one gets the set of equations

$$M_{pp}\,\Phi^p + M_{pw}\,\Phi^w + M_{pc}\,I^c = -R_{p\xi}\,\xi, \tag{15}$$

$$\begin{aligned}\frac{d}{dt}(M_{wp}\,\Phi^p + M_{ww}\,\Phi^w + M_{wc}\,I^c) &= -\frac{1}{\sigma d}N_{ww}\,\Phi^w,\\ \frac{d}{dt}(M_{cp}\,\Phi^p + M_{cw}\,\Phi^w + M_{cc}\,I^c) &= -R_c\,I^c + U^{feedb}_c.\end{aligned} \tag{16}$$

The open-loop problem is defined by the set of equations with $U^{feedb}_c = 0$.

The closed-loop problem can be formulated by setting

$$U^{feedb}_c = G^1_{cS}\,b_S + G^2_{cS}\,\frac{d}{dt}b_S\,, \qquad b_S = b_{Sp}\,\Phi^p + b_{Sw}\,\Phi^w + b_{Sc}\,I^c \tag{17}$$

where G^1_{cS}, G^2_{cS} are gain or amplification matrices and $b_S = \{b_{s_1}, b_{s_2},\ldots\}$ are magnetic sensor signals produced by the currents of the system.

Eliminating Φ^p by solving eq. (15) for Φ^p gives

$$\Phi^p = -M^{-1}_{pp}M_{pw}\Phi^w - M^{-1}_{pp}M_{pc}I^c - M^{-1}_{pp}R_{p\xi}\xi. \tag{18}$$

Substituting (18) into (14) yields

$$\begin{pmatrix}\mathbf{M}_{XX} & \mathbf{M}_{X\xi}\\ \mathbf{M}_{\xi X} & \mathbf{M}_{\xi\xi} + M_{\xi p}M^{-1}_{pp}R_{p\xi}\end{pmatrix}\cdot\begin{pmatrix}X\\ \xi\end{pmatrix} = \begin{pmatrix}0\\ (M_{\xi c} - M_{\xi p}M^{-1}_{pp}M_{pc})I^c + (M_{\xi w} - M_{\xi p}M^{-1}_{pp}M_{pw})\Phi^w\end{pmatrix} \tag{19}$$

or , when solved for ξ,

$$\xi = M_{\xi\ c+w}\ \begin{pmatrix}I^c\\ \Phi^w\end{pmatrix}. \tag{20}$$

Inserting (18) and (20) in eqs. (16) one gets a set of linear equations defining an initial

value problem of first order in time. Assuming a time dependence $e^{\gamma t}$, the normal modes of the system are obtained by solving the generalized eigenvalue problem

$$\begin{aligned}
&\gamma\left[\begin{pmatrix} \widetilde{M}_{cc} & \widetilde{M}_{cw} \\ \widetilde{M}_{wc} & \widetilde{M}_{ww} \end{pmatrix} - \begin{pmatrix} \widetilde{M}_{c\xi}\cdot M_{\xi c+w} \\ \widetilde{M}_{w\xi}\cdot M_{\xi c+w} \end{pmatrix} - \begin{pmatrix} G^2_{cS}\widetilde{b}_{Sc+w} \\ 0 \end{pmatrix}\right]\begin{pmatrix} I^c \\ \Phi^w \end{pmatrix} \\
= &\left[-\begin{pmatrix} R_c & 0 \\ 0 & \frac{1}{\sigma d}N_{ww} \end{pmatrix} + \begin{pmatrix} G^1_{cS}\widetilde{b}_{Sc+w} \\ 0 \end{pmatrix}\right]\begin{pmatrix} I^c \\ \Phi^w \end{pmatrix},
\end{aligned} \tag{21}$$

$$\begin{aligned}
\widetilde{M}_{cc} &= M_{cc} - M_{cp}M_{pp}^{-1}(M_{pc} + R_{p\xi}M_{\xi c}) \\
\widetilde{M}_{cw} &= M_{cw} - M_{cp}M_{pp}^{-1}(M_{pw} + R_{p\xi}M_{\xi w}) \\
\widetilde{M}_{wc} &= M_{wc} - M_{wp}M_{pp}^{-1}(M_{pc} + R_{p\xi}M_{\xi c}) \\
\widetilde{M}_{ww} &= M_{ww} - M_{wp}M_{pp}^{-1}(M_{pw} + R_{p\xi}M_{\xi w}),
\end{aligned} \tag{22}$$

$$b_S = \underbrace{(b_{Sc} - b_{Sp}M_{pp}^{-1}M_{pc})}_{\widetilde{b}_{Sc}} I^c + \underbrace{(b_{Sw} - b_{Sp}M_{pp}^{-1}M_{pw})}_{\widetilde{b}_{Sw}} \Phi^w - \underbrace{b_{Sp}M_{pp}^{-1}R_{p\xi}}_{\widetilde{b}_{S\xi}} \xi, \tag{23}$$

$$\widetilde{b}_{Sc+w} = (\widetilde{b}_{Sc} + \widetilde{b}_{Sw}) - \widetilde{b}_{S\xi}M_{\xi c+w}. \tag{24}$$

The STARWALL code solves this problem numerically. The potential plasma energy $W_p(\xi,\xi)$ is provided by the CAS3D stability code [2], the equilibrium by the VMEC code [3]. For faster wall modes the open-loop problem can be solved with an extended version of the CAS3D code, in which the kinetic energy of the plasma perturbation is taken into account [4].
The problem remains to find the best available feedback logics, i. e., to make an optimal choice of the numerous elements of the gain matrices G^1_{cS} and G^2_{cS}. To simplify this problem, these matrices are assumed to be linear combinations of a few, skillfully predefined basic matrices:

$$G^1_{cS} = \sum_{i=1}^{N_\alpha} \alpha_i G^1_{cS,i}, \qquad G^2_{cS} = \sum_{i=1}^{N_\beta} \beta_i G^2_{cS,i}. \tag{25}$$

The coefficients α_i and β_i are free, variable design parameters. To make a good choice for them, the eigenvalue optimization code OPTIM has been developed. Its principle is described in the following.
Substituting (25) into the closed loop stability problem (21), one finds that it takes the form

$$\mathbf{A}\mathbf{x} = \gamma\mathbf{B}\mathbf{x}, \tag{26}$$

whith $\mathbf{x} = (I^c, \Phi^w)^T$ being the system's state vector. The $M \times M$ matrices $\mathbf{A}$ and $\mathbf{B}$ are decomposed as

$$\mathbf{A} = \mathbf{A}_0 + \sum_{i=1}^{N_\alpha} \alpha_i \mathbf{A}_i, \qquad \mathbf{B} = \mathbf{B}_0 + \sum_{i=1}^{N_\beta} \beta_i \mathbf{B}_i, \tag{27}$$

where $\mathbf{A}_0$ and $\mathbf{B}_0$ are the open loop contributions, $\mathbf{A}_i$, $i = 1,\ldots,N_\alpha$ the "proportional gain" feedback matrices, and $\mathbf{B}_i$, $i = 1,\ldots,N_\beta$ the "derivative gain" feedback matrices. Assuming that $\mathbf{B}$ is invertible, (26) is equivalent to the ordinary, parametrized eigenvalue problem

$$\mathbf{B}^{-1}\mathbf{A}\mathbf{x} = \gamma\mathbf{x}, \tag{28}$$

yielding the eigenvalues γ_j, $j = 1, \ldots, M$. Feedback stabilization is achieved when a set of parameters α_i and β_i is found such that $\mathrm{Re}(\gamma_j) < 0$ for all j. To determine such parameter sets automatically, the OPTIM code minimizes either the so called spectral abscissa $\mathcal{F}_1$ or the "exponential spectral function" $\mathcal{F}_2$,

$$\mathcal{F}_1(\gamma_1, \ldots, \gamma_M) = \max_{j=1,\ldots,M} \mathrm{Re}\,\gamma_j, \qquad \mathcal{F}_2(\gamma_1, \ldots, \gamma_M) = \sum_{j=1}^{M} \exp(\mathrm{Re}\,\gamma_j) \tag{29}$$

under variations of α_i, $i = 1, \ldots, N_\alpha$ and β_i, $i = 1, \ldots, N_\beta$. Optimization of $\mathcal{F}_1$ gives the best achievable asymptotic stability of the system, whereas minimization of $\mathcal{F}_2$ results in a faster decay of transient disturbances.
Let $\mathcal{F}$ be either $\mathcal{F}_1$ or $\mathcal{F}_2$, and $\tilde{\mathcal{F}}(\alpha_1, \ldots, \alpha_{N_\alpha}, \beta_1, \ldots, \beta_{N_\beta}) = \mathcal{F}(\gamma_1(\{\alpha_i\}, \{\beta_i\}), \ldots, \gamma_M(\{\alpha_i\}, \{\beta_i\}))$. For the numerical efficiency of minimizing $\tilde{\mathcal{F}}$, it is highly beneficial to provide an analytic expression for its gradient:

$$\frac{\partial \tilde{\mathcal{F}}}{\partial \alpha_i} = \sum_{j=1}^{M} \frac{\partial \mathcal{F}}{\partial \gamma_j} \frac{\partial \gamma_j}{\partial \alpha_i}, \qquad \frac{\partial \tilde{\mathcal{F}}}{\partial \beta_i} = \sum_{j=1}^{M} \frac{\partial \mathcal{F}}{\partial \gamma_j} \frac{\partial \gamma_j}{\partial \beta_i}. \tag{30}$$

The derivatives $\partial \mathcal{F} / \partial \gamma_j$ are easy to determine. But there also exist analytic formulas for $\partial \gamma_j / \partial \alpha_i$ and $\partial \gamma_j / \partial \beta_i$, which can be derived by means of first-order perturbation theory, cf. [5]. Despite the existence of an analytic gradient, the optimization procedure is feasible with today's computational resources only if the matrices $\mathbf{A}_i$, $\mathbf{B}_i$ can be substantially reduced in size. To this end, each matrix is first subjected to a similarity transform of the form $\mathbf{M}' = \mathbf{X}^T \mathbf{M} \mathbf{X}$, where $\mathbf{M} = \mathbf{A}_i$, $\mathbf{B}_i$, and the columns of $\mathbf{X}$ contain the orthonormal open loop eigenvectors, sorted according to descending order of the respective eigenvalues:

$$\mathbf{X} = (\mathbf{x}_1, \ldots, \mathbf{x}_M), \quad \mathbf{B}_0^{-1} \mathbf{A}_0 \mathbf{x}_j = \gamma_j \mathbf{x}_j, \quad \gamma_j > \gamma_{j+1}\ \forall j = 1, \ldots, M-1. \tag{31}$$

Afterwards, the system is projected onto the least stable eigenvectors, i. e., only an upper left quadratic matrix block with $\mathcal{O}(100)$ rows and columns is accounted for, respectively. The optimization procedure is applied to this reduced system. At last, as a cross-check, the resulting optimal parameter values α_i, β_i are substituted into the full-sized closed loop system, and the corresponding eigenvalue problem is solved. It is often found that the matrix truncation hardly affects the leading eigenvalues if the reduced matrices are still sufficiently large.
Conventional algorithms for nonlinear optimization usually fail when attempting to minimize spectral functions like (29). This is due to the fact that such functions are likely to be non-smooth or even non-Lipschitz, i. e., there exist manifolds in parameter space where the gradient diverges. Adapted from [6], the OPTIM code includes a so called gradient bundle method which can cope with such malicious kind of functions.

3. Application

The numerical procedure has been applied to an ASDEX-Upgrade type equilibrium. The equilibrium has been calculated with the VMEC code [3]. The magnetic surfaces, the q-profile and the pressure are shown in FIG. 1a-b. The equilibrium with an average $< \beta > = 0.03$ is $n = 1$ external kink unstable without a stabilizing conducting wall. The Fourier harmonics of the normal displacement $\xi^s_{mn} (\equiv odd), \xi^c_{mn} (\equiv even)$ of the unstable $(n = 1)$ eigenfunction obtained with the CAS3D stability code are plotted in FIG. 2.

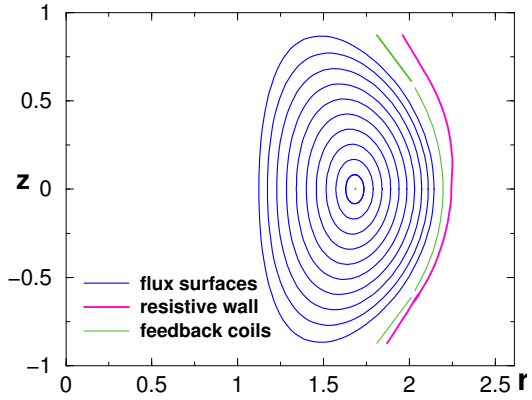

FIG. 1a

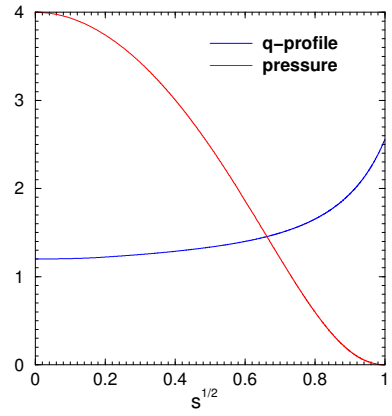

FIG. 1b

FIG. 1a-b Flux-surfaces, q-profile and pressure of an ASDEX Upgrade type equilibrium: $< \beta >= 0.03$

The mode can be stabilized by an ideally conducting wall $(\sigma = \infty)$ sufficiently close to the plasma boundary. The equilibrium has been found to be stable by applying the multiply connected wall shown in FIG. 5a. The wall configuration is a preliminary design for ASDEX Upgrade. For non-zero wall resistance $(\sigma \neq \infty)$ the equilibrium becomes again unstable. Running the STARWALL code in the open-loop mode two unstable $(n = 1)$ eigenvalues are obtained: $\gamma\mu_0\sigma d = 7.45$ and $\gamma\mu_0\sigma d = 5.83$. In FIG. 4 the m-harmonics of the normal displacement of the unstable modes at the plasma boundary and in FIG. 3 the growth rate versus resistance $1/(\sigma d)$ of the most unstable mode is shown. In order to stabilize the modes, a feedback configuration has been chosen taking into account the proportional gain matrix only. Poloidal field sensor signals were taken from $n_{se} = 8$ sensors located at the center of the central coil set (FIG. 5b).

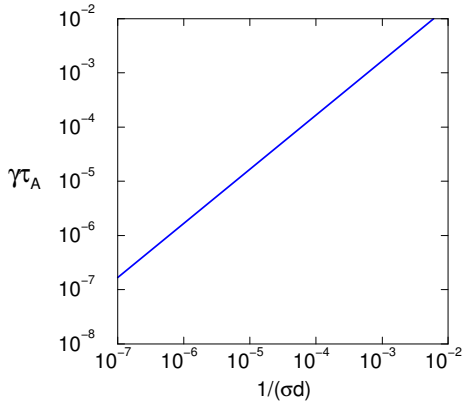

FIG. 3 Growth rate of the $(n = 1)$ *resistive wall mode versus* $1/(\sigma d)$*, magnetic field* $B_0 = 2.64$ *T, major radius* $R = 1.57m$*,* $\tau_A =$ *Alfvén time.*

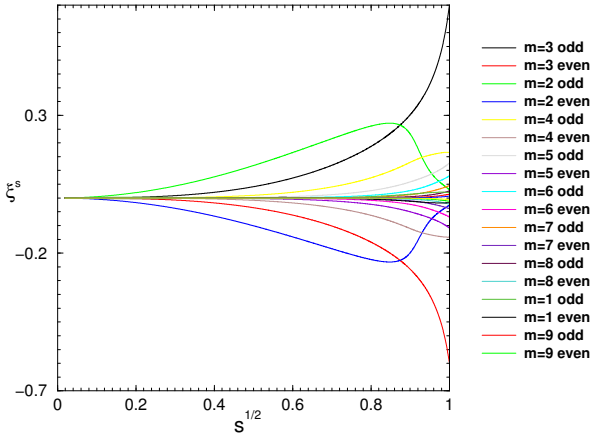

FIG. 2 m-harmonics of the $(n=1)$ *external kink mode without conducting wall*

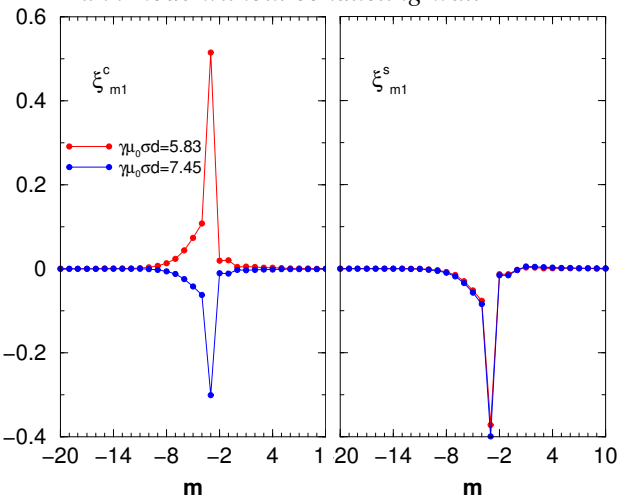

FIG. 4 m-harmonics of the normal displacement at the plasma boundary of the $(n=1)$ *resistive eigenmodes.*

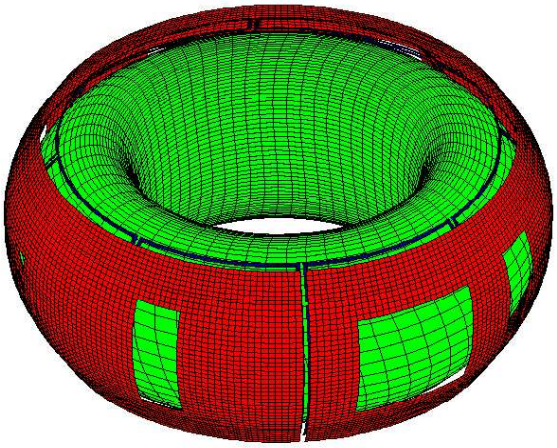

FIG. 5a

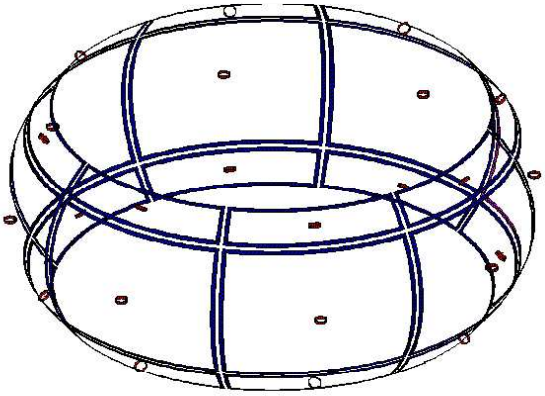

FIG. 5b

FIG. 5a-b Design of a stabilizing wall for ASDEX Upgrade, 3 sets of 8 feedback coils and sensor positions are shown. Discretisation of the wall: $n_t^w = 19182$ *triangles and of the plasma boundary:* $n_u = 192$ *poloidal mesh-points,* $n_v = 96$ *toroidal mesh-points,* $n_t^p = 36864$ *triangles*

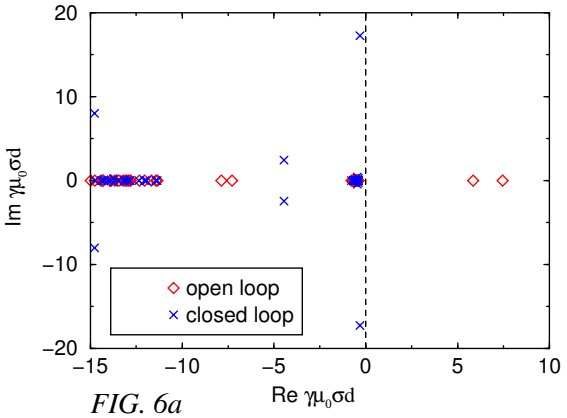

FIG. 6a

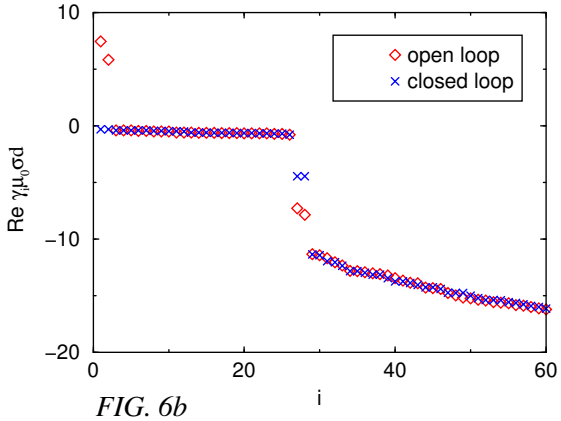

FIG. 6b

FIG. 6a-b Complex eigenvalues (a) and the real part of the first 60 eigenvalues in decreasing order (b) of the open- and closed-loop solution, total number of eigenvalues computed $n_e = 9074$

Anticipating the toroidal $(n = 1)$ mode structure of the perturbation a gain matrix with 6 free parameters has been defined

$$G^1_{c,S,i,k} = p^s_l \sin\left(\frac{2\pi}{n_{se}}(j-k)\right) + p^c_l \cos\left(\frac{2\pi}{n_{se}}(j-k)\right), \quad \begin{matrix} i = j + n_{se}l, j = 1, n_{se}, l = 0, 2, \\ k = 1, n_{se}, \end{matrix}$$

$0 < i \leq n_{se}$: central , $n_{se} < i \leq 2n_{se}$: upper , $2n_{se} < i \leq 3n_{se}$: lower coil set.

Running the optimization procedure a stable configuration has been obtained with the parameter: $p^s_0 = -18.5$, $p^c_0 = -11.4$, $p^s_1 = 9.8$, $p^c_1 = 14.3$, $p^s_2 = -37.6$, $p^c_2 = -29.5$. For the feedback coil resistance it was assumed $R^c = 0.01\frac{1}{\sigma d}$, $\frac{1}{\sigma d}$ = wall resistance. In FIG. 6a-b the leading parts of the eigenvalue spectrum of the open- and closed-loop solution are shown.

4. References

[1] CHU M.S. et al, Nucl. Fusion **43** (2003) 441
[2] NÜHRENBERG C., Phys. Plasmas **3** (1996) 240
[3] HIRSHMAN S.P. et al, Phys. Fluids **28** (1985) 1387
[4] MERKEL P. et al, 31st EPS Conf. on Plasma Phys., (2004), ECA Vol. **28B**, P-1.208
[5] HORN,C. A. et al. ,Matrix Analysis, Cambridge University Press, Cambridge(1985)
[6] BURKE,R. A. et al.,Lin. Algebra Appl.,(2002), **351-352**, 117-145